mmi_6956

Molecular Microbiology (2009) ■

doi:10.1111/j.1365-2958.2009.06956.x

Quaternary structure changes in a second Per-Arnt-Sim domain mediate intramolecular redox signal relay in the NifL regulatory protein

Peter Slavny,[1] Richard Little,[1] Paloma Salinas,[1†] Thomas A. Clarke[2] and Ray Dixon[1*]

[1]*Department of Molecular Microbiology, John Innes Centre, Norwich, NR4 7UH, UK.*

[2]*School of Biological Sciences, University of East Anglia, Norwich Research Park, Norwich, NR4 7TJ, UK.*

Summary

Per-Arnt-Sim (PAS) domains play a critical role in signal transduction in multidomain proteins by sensing diverse environmental signals and regulating the activity of output domains. Multiple PAS domains are often found within a single protein. The NifL regulatory protein from *Azotobacter vinelandii* contains tandem PAS domains, the most N-terminal of which, PAS1, contains a FAD cofactor and is responsible for redox sensing, whereas the second PAS domain, PAS2, has no apparent cofactor and its function is unknown. Amino acid substitutions in PAS2 were identified that either lock NifL in a form that constitutively inhibits NifA or that fail to respond to the redox status, suggesting that PAS2 plays a pivotal role in transducing the redox signal from PAS1 to the C-terminal output domains. The isolated PAS2 domain is a homodimer in solution and the subunits are in rapid exchange. PAS2 dimerization is maintained in the redox signal transduction mutants, but is inhibited by substitutions in PAS2 that lock NifL in the inhibitory conformer. Our results support a model for signal transduction in NifL, whereby redox-dependent conformational changes in PAS1 are relayed to the C-terminal domains via changes in the quaternary structure of the PAS2 domain.

Introduction

Per-ARNT-Sim (PAS) domains are ubiquitous signalling modules found in all kingdoms of life. They can detect a plethora of stimuli including light, oxygen, redox potential, proton motive force and various small molecules as well as modulating protein–protein interactions (Taylor and Zhulin, 1999). Despite a poorly conserved primary amino acid sequence, PAS domains are structurally homologous and are characterized by a conserved α/β fold consisting of approximately 110 amino acids (Taylor and Zhulin, 1999). The PAS domains can bind a variety of cofactors including FAD, FMN, [4Fe-4S] clusters, haeme and 4-hydroxycinnamic acid. Detection of environmental changes by these moieties often induces a change in the quaternary structure of the PAS domain. The importance of this structural plasticity with respect to signalling has been recently demonstrated in several systems (Möglich and Moffat, 2007; Ayers and Moffat, 2008; Lee *et al.*, 2008; Nakasone *et al.*, 2008; Zoltowski and Crane, 2008; Evans *et al.*, 2009; Scheuermann *et al.*, 2009). For example, the cLOV domain (a FMN-containing PAS domain from the light-sensing YtvA protein) forms a stable dimer and signal detection induces a change in the symmetry of this dimer in which the subunits undergo a 5° rotation with respect to one another (Möglich and Moffat, 2007).

Multiple PAS domains can often be found in tandem within a single protein. Despite the abundance of duplicate PAS domains, the role of these multiple domains in signal perception and transduction has only been analysed in relatively few cases. The biological function of duplicate PAS domains is often unclear due to the apparent lack of any cofactor or ligand binding pocket that might be indicative of a role in signal perception (Etzkorn *et al.*, 2008; Lee *et al.*, 2008). A well-studied example is *Azotobacter vinelandii* NifL, a redox-sensing regulatory protein that contains two PAS domains in tandem. The most N-terminal of these (PAS1) binds a FAD cofactor and is required for redox sensing (Hill *et al.*, 1996; Macheroux *et al.*, 1998; Söderbäck *et al.*, 1998) whereas the second PAS domain of NifL (PAS2) has no apparent cofactor and its function is unknown.

NifL regulates the transcription of *nif* genes (required for the biosynthesis and activity of molybdenum-dependent nitrogenase) in *A. vinelandii* via interactions with the transcriptional activator NifA. When environmental

Accepted 2 November, 2009. *For correspondence. E-mail ray.dixon@bbsrc.ac.uk; Tel. (+44) 1603 450747; Fax (+44) 1603 450778. †Present address: División de Genética, Universidad de Alicante Apdo. 99 03080 Alicante, Spain.

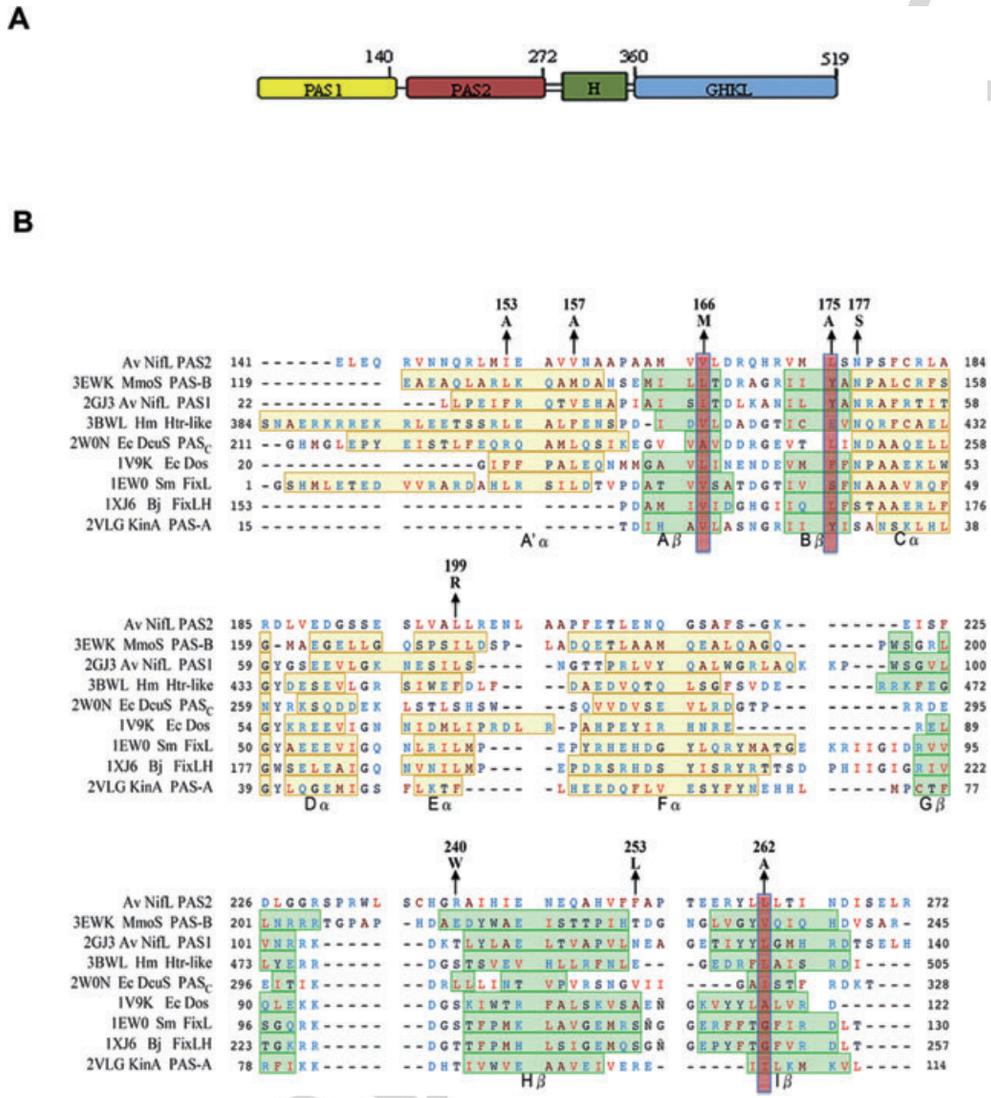

6 **Fig. 1.** Domain structure of NifL and PAS2 sequence alignment.
A. Domain structure of *A. vinelandii* NifL (Uniprot code P30663).
B. Sequence alignment of the *A. vinelandii* PAS2 domain with PAS domains of known structure (PDB code and protein designation are listed to the left of each sequence). α-Helices are highlighted in yellow and β sheets in green. Residues in the conserved PAS dimer interface (Ayers and Moffat, 2008) are highlighted in orange. Amino acid substitutions in *A. vinelandii* PAS2 analysed in this study are indicated by arrows above the text.

circumstances do not favour nitrogen fixation, NifL inhibits NifA activity via formation of a protein–protein complex. The stability of this complex, and thus the activity of NifA, is controlled by NifL in response to the redox status of the cell and the availability of fixed nitrogen (Schmitz *et al.*, 2002; Dixon and Kahn, 2004; Martinez-Argudo *et al.*, 1 2004a). In addition to the N-terminal PAS domains, the *A. vinelandii* NifL protein contains two other discrete domains: an H domain that shares homology with the HisKA domains of the histidine protein kinases (Little *et al.*, 2007) and a C-terminal nucleotide binding domain belonging to the GHKL superfamily of ATPases (Perry *et al.*, 2005) (Fig. 1A). The GHKL domain binds adenosine nucleotides and mediates nitrogen sensing via an interaction with the GlnK signal transduction protein (Little *et al.*, 2000; 2002; Rudnick *et al.*, 2002) while the H domain is thought to provide an interaction surface for NifA binding (Little *et al.*, 2007). Our understanding of redox sensing by NifL is enhanced by the availability of the crystal structure of the PAS1 domain, which reveals an extensive hydrogen-bonding network involving the FAD cofactor, several co-ordinating residues and two embed-

ded water molecules (Key *et al*., 2007). This hydrogen-bonding network may be sensitive to changes in the redox state of the FAD group and it has been postulated that re-organization of this network constitutes the initial structural change associated with redox signal perception (Key *et al*., 2007). This structural signal must somehow be propagated or amplified in order to trigger a conformational change in NifL that promotes inhibition of NifA activity. However, the molecular mechanism by which signal perception by PAS1 is coupled to conformational changes in the C-terminal domains of the protein to mediate the interaction with NifA is unknown.

As mentioned above, the function of the second PAS domain of NifL (PAS2) has not so far been defined. In this study we have used a combination of genetic and biochemical approaches to analyse the role of this second PAS domain in signalling. Our results suggest that NifL PAS2 undergoes a shift in quaternary structure in response to the detection of redox signals by the PAS1 domain. This structural change in PAS2 modulates NifL activity and is important for intramolecular redox signal relay. These findings highlight the importance of the plasticity of PAS domain quaternary structure in the signalling mechanism.

Results

Mutagenesis of the PAS2 domain of NifL

The region of NifL located between residues 151–268 is recognized as a PAS domain in the SMART and PFAM databases. We designate this domain as PAS2 to distinguish it from the well-characterized FAD-containing redox sensory domain, PAS1 (Fig. 1). Secondary structure predictions using the PSIPRED server and alignments with known PAS structures indicate that PAS2 is likely to contain structural elements found in other PAS domains (Fig. 1). In order to investigate the function of PAS2 in signal transduction, we generated alanine substitutions in residues predicted to be located in the conserved dimerization interface that includes an N-terminal alpha helix (A′α) and extends throughout the β-sheets in known PAS structures (Ayers and Moffat, 2008). We also randomly mutagenized the sequence encoding PAS2 using error-prone PCR and inserted the mutant library into *nifL* to replace the wild-type sequence. The resultant NifL mutants were screened for differences in their ability to inhibit NifA activity in *Escherichia coli* using a two-plasmid system consisting of a reporter plasmid carrying a *nifH–lacZ* fusion, and a second plasmid from which *nifL* and *nifA* are cotranscribed under the control of a constitutive promoter (Söderbäck *et al*., 1998; Reyes-Ramirez *et al*., 2002). In this system nitrogen regulation is conveyed by the interaction of *E. coli* PII signal transduction proteins with NifL (Little *et al*., 2000; Reyes-Ramirez *et al*., 2001). Colonies expressing wild-type NifL are pale blue on Xgal indicator plates containing limiting fixed nitrogen when incubated under aerobic conditions. We screened for mutants that appeared white (indicating enhanced repression of NifA activity by NifL) or dark blue (suggesting the NifL mutant protein was deficient in its ability to inhibit NifA). Two phenotypes emerged from both the random and site-directed approaches; 'locked-on' mutants that inhibited NifA constitutively, and 'redox signalling' mutants that failed to respond to the presence of oxygen but inhibited NifA in the presence of high levels of fixed nitrogen. The positions of all amino acid substitutions belonging to these categories are indicated in Fig. 1.

'Locked-on' mutations

Seven mutations in the PAS2 domain were identified that result in inhibition of NifA activity irrespective of environmental conditions. This contrasts with wild-type NifL, which represses NifA activity in discrete responses to oxygen (Fig. 2A, compare the solid black and open bars) and fixed nitrogen (Fig. 2A, compare black and horizontally striped bars) or a combination of both (Fig. 2A, grey bars) as demonstrated previously (Söderbäck *et al*., 1998; Reyes-Ramirez *et al*., 2002). Control experiments demonstrated that there is no transcription from the reporter fusion in the absence of NifA (Fig. 2A, bars marked 'Reporter only') and that NifA is active across all four conditions in the absence of regulation by its partner protein, NifL (Fig. 2A, bars marked 'NifA'). The amino acid substitutions V157A, V166M, L175A, N177S, L199R, R240W and L262A apparently lock the NifL protein in the inhibitory conformer. These substitutions are dispersed throughout the PAS2 domain and their positions in the predicted secondary structure are indicated in Fig. 1. All of the 'locked-on' variant proteins were stable under the four growth conditions tested, as assessed by Western blotting (data not shown).

It has previously been shown that NifL requires nucleotide binding to the C-terminal GHKL domain in order to inhibit NifA activity. NifL is incompetent to bind NifA *in vitro* in the absence of nucleotide and the binding of ADP to the GHKL domain has been shown to stabilize the NifL-NifA binary complex (Eydmann *et al*., 1995; Money *et al*., 1999). Mutations in the GHKL domain that prevent binding of adenosine nucleotides result in the inability of NifL to inhibit NifA *in vivo* (Martinez-Argudo *et al*., 2004b; Perry *et al*., 2005). To assess whether the 'locked-on' phenotype of the PAS2 mutations requires nucleotide binding, the substitutions were combined with a second amino acid substitution in the GHKL domain (G480A), which has been fully characterized in previous studies, and is known to disrupt ADP binding (Perry *et al*., 2005). Data for

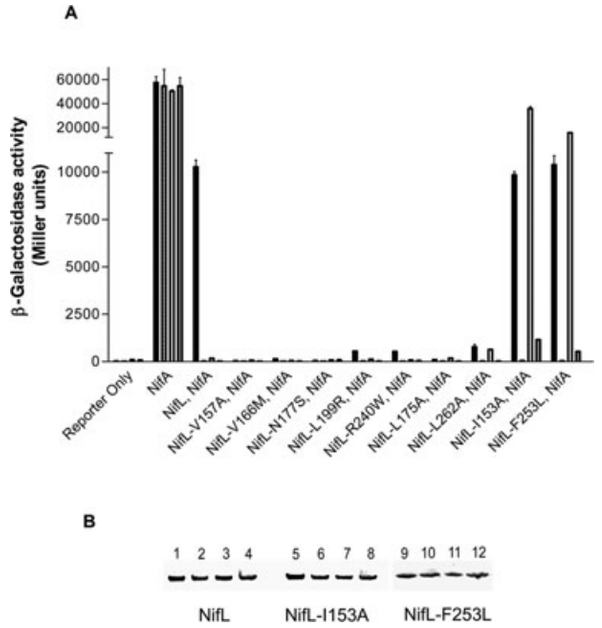

Fig. 2. Activity and stability of mutant NifL proteins *in vivo*.
A. Influence of mutant NifL proteins on transcriptional activation by NifA *in vivo*. Cultures were grown under the following conditions; anaerobically, under nitrogen-limiting conditions with casein hydrolysate as the sole nitrogen source (black bars), anaerobically with $(NH_4)_2SO_4$ as nitrogen source (horizontally striped bars), aerobically with casein hydrolysate as nitrogen source (white bars) and aerobically with $(NH_4)_2SO_4$ as nitrogen source (grey bars). Cultures were assayed for β-galactosidase activity as a reporter of NifA-mediated transcriptional activation from the *nifH–lacZ* fusion on plasmid pRT22 as described previously (Söderbäck *et al*., 1998; Reyes-Ramirez *et al*., 2001; Martinez-Argudo *et al*., 2004c). All experiments were performed at least in duplicate with error bars denoting the standard error of the mean.
B. Western analysis of the wild-type and mutant NifL proteins in strains grown under the same four conditions as used for the β-galactosidase assays.

V166M are shown in Table 1 and similar results were observed with L199R (data not shown). The presence of the additional G480A substitution severely compromised the ability of the V166M variant to inhibit NifA (Table 1, compare rows 4 and 6) and hence the G480A mutation is dominant over V166M. This implies that the 'locked-on' PAS2 mutants are similar to the wild type in their requirement for nucleotide binding to the GHKL domain to achieve inhibition of NifA activity. In contrast, substitutions in the H domain of NifL that give rise to a 'locked-on' phenotype exhibit a decreased requirement for nucleotide binding *in vitro* and are dominant to the G480A substitution *in vivo* (Martinez-Argudo *et al*., 2004b).

The redox sensing PAS1 domain of NifL is required for the inhibition of NifA activity in response to oxygen (Söderbäck *et al*., 1998). To investigate whether input from the PAS1 domain is necessary to maintain the 'locked-on' phenotype of the PAS2 substitutions, we introduced the V166M mutation into a truncated form of NifL that lacks PAS1, $NifL_{(143–519)}$. As demonstrated previously (Söderbäck *et al*., 1998), this truncated form of NifL does not inhibit NifA in response to oxygen, but responds normally to the addition of fixed nitrogen (Table 2, row 5). However, when the V166M substitution was present in the truncated protein lacking PAS1, constitutive inhibition of NifA activity was retained (Table 2, compare rows 4 and 6), suggesting that the 'locked-on' phenotype of the PAS2 mutations is independent of the PAS1 domain.

'Redox signalling' mutations in the PAS2 domain of NifL

We have identified two mutations in the PAS2 domain that give rise to a form of the NifL protein that is insensitive to redox signals but responds normally to fixed nitrogen. In contrast to wild-type NifL, which strongly represses NifA activity in response to oxygen (Fig. 2A), the variants NifL-I153A and NifL-F253L allow high levels of NifA activity under oxidizing conditions (Fig. 2A, white bars), while retaining the ability to inhibit NifA activity in response to fixed nitrogen (Fig. 2A, compare the white and grey bars). The mutant proteins appear to be stable under all conditions tested, as detected by Western blotting (Fig. 2B).

The residues I153 and F253 are located in the predicted A′α helix and the Hβ sheet of the PAS2 domain respectively (Fig. 1). PAS2 has no apparent role in perception of

Table 1. The 'locked-on' phenotype of the V166M substitution requires a functional nucleotide-binding (GHKL) domain.

			β-Galactosidase activity in Miller Units (± SE)			
			Anaerobic		Aerobic	
Row	Plasmid	Protein(s)	N–	N+	N–	N+
1	–	Reporter only	90 (± 3)	37 (± 14)	154 (± 2)	30 (± 4)
2	pPR39	NifA	85217 (± 5551)	203320 (± 35830)	80003 (± 2503)	81818 (± 6504)
3	pPR34	NifA, NifL	6115 (± 833)	97 (± 3)	279 (± 0)	51 (± 2)
4	pPS20	NifA, NifL-V166M	304 (± 2)	18 (± 18)	163 (± 7)	42 (± 2)
5	pNLG480A	NifA, NifL-G480A	86563 (± 634)	90943 (± 328)	58257 (± 9595)	41418 (± 3754)
6	pPS124	NifA, NifL-V166M, G480A	93644 (± 3153)	33592 (± 2757)	66683 (± 4086)	8108 (± 462)

Table 2. The PAS1 domain is not required for the 'locked-on' phenotype of the V166M substitution.

			β-Galactosidase activity in Miller Units (± SE)			
			Anaerobic		Aerobic	
Row	Plasmid	Protein(s)	N–	N+	N–	N+
1	–	Reporter only	15 (± 0)	19 (± 2)	124 (± 15)	99 (± 8)
2	pPR39	NifA	25004 (± 9693)	150911 (± 3301)	48843 (± 2037)	59216 (± 2837)
3	pPR34	NifA, NifL	12583 (± 546)	28 (± 2)	221 (± 10)	93 (± 15)
4	pPS20	NifA, NifL-V166M	547 (± 24)	16 (± 1)	114 (± 24)	21 (± 8)
5	pPS54	NifA, $NifL_{(143–519)}$	12423 (± 471)	93 (± 5)	7347 (± 286)	565 (± 12)
6	pPS77	NifA, $NifL_{(143–519)}$-V166M	1166 (± 57)	17 (± 0.3)	609 (± 32)	47 (± 6)

redox signals as $NifL_{(143–519)}$ (which contains the PAS2, H and GHKL domains) is not redox responsive (Table 2, row 5) and no cofactor is evident in either $NifL_{(143–519)}$ or the isolated PAS2 domain itself (••, unpubl. data). Therefore, the presence of mutations in PAS2 that perturb the redox response implies that this domain has a role in signal relay from the redox sensing PAS1 domain to the C-terminal domains of NifL.

Effect of substitutions on the quaternary structure of the PAS2 domain

The PAS domains are often dimeric in solution (Erbel *et al*., 2003; Card *et al*., 2005; Lee *et al*., 2008; Zoltowski and Crane, 2008) and several of the crystal structures solved to date are dimers in the asymmetric unit (Ma *et al*., 2008). Moreover, there is evidence that the quaternary structure of PAS domains is important for signalling in several systems (Möglich and Moffat, 2007; Etzkorn *et al*., 2008; Lee *et al*., 2008; Zoltowski and Crane, 2008; Evans *et al*., 2009). The bacterial adenylate cyclase two-hybrid (BACTH) system (Karimova *et al*., 1998) was used to analyse self-association between isolated subunits of the NifL PAS2 domain. We detected an interaction in the BACTH system between wild-type PAS2 domains (Fig. 3, bars marked 'WT'), indicating that the domain is multimeric. All 'locked-on' substitutions tested perturbed this interaction (Fig. 3, compare black bars marked 'WT' with those marked 'N177S', 'V157A', 'V166M', 'L175A' and 'L262A'). By contrast the mutants defective in redox signalling were competent to maintain the interaction (Fig. 3, compare 'WT' with 'I153A' and 'F253L'). These results suggest that the 'locked-on' mutations may influence activity by disrupting oligomerization of the PAS2 domain.

To investigate this possibility further, the isolated PAS2 domain (NifL residues 143–284) and its mutants were expressed with an N-terminal his-tag and purified by nickel affinity chromatography. The oligomerization state of the PAS2 domain and mutant derivatives in solution was analysed by size exclusion chromatography (Fig. 4).

When loaded onto the gel filtration column the wild-type PAS2 domain eluted in a single peak with an apparent molecular mass somewhat lower than that predicted for a spherical dimeric species (38.56 kDa). Retention volumes were clearly concentration-dependent within the range 26–519 μM (Fig. 4A), with apparent molecular weights ranging from 32.3 to 37.2 kDa (Table S1). The concentration dependence of the elution profile suggests rapid interconversion between the monomer and dimer forms during the timescale of the chromatography. The F253L substitution, which gives rise to a 'redox signalling' phenotype in the full-length protein, exhibited similar elution profiles to that of the wild-type PAS2 domain (Fig. 4C). The I153A substituted domain also eluted as a dimer on gel filtration (Fig. 4B), but the profile was less concentration-dependent than the wild-type PAS2 domain and above

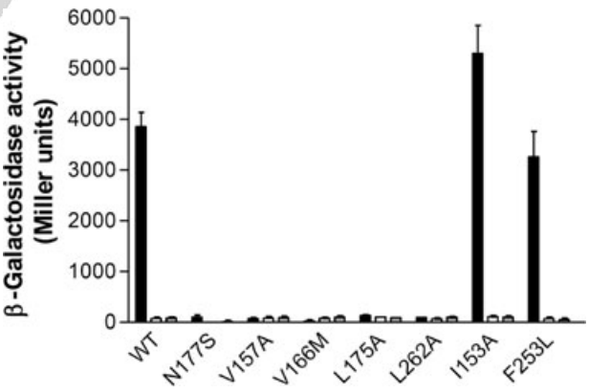

Fig. 3. BACTH analysis of PAS2 oligomerization. Hybrid proteins containing the T18 or T25 subunit of adenylate cyclase fused to the NifL PAS2 domain (NifL residues 147–284) or mutant variants of NifL PAS2 were constructed and expressed as described in *Experimental Procedures*. Each NifL variant is shown as a block of three bars: black bars represent interactions between two-hybrid proteins while the white and grey bars are controls in which the T18-PAS2 fusion protein is expressed with the T25 subunit only (white bars) or the T25-PAS2 fusion protein is expressed with the T18 subunit only (grey bars). Graphs show an average of at least two replicates and error bars indicate the standard error of the mean.

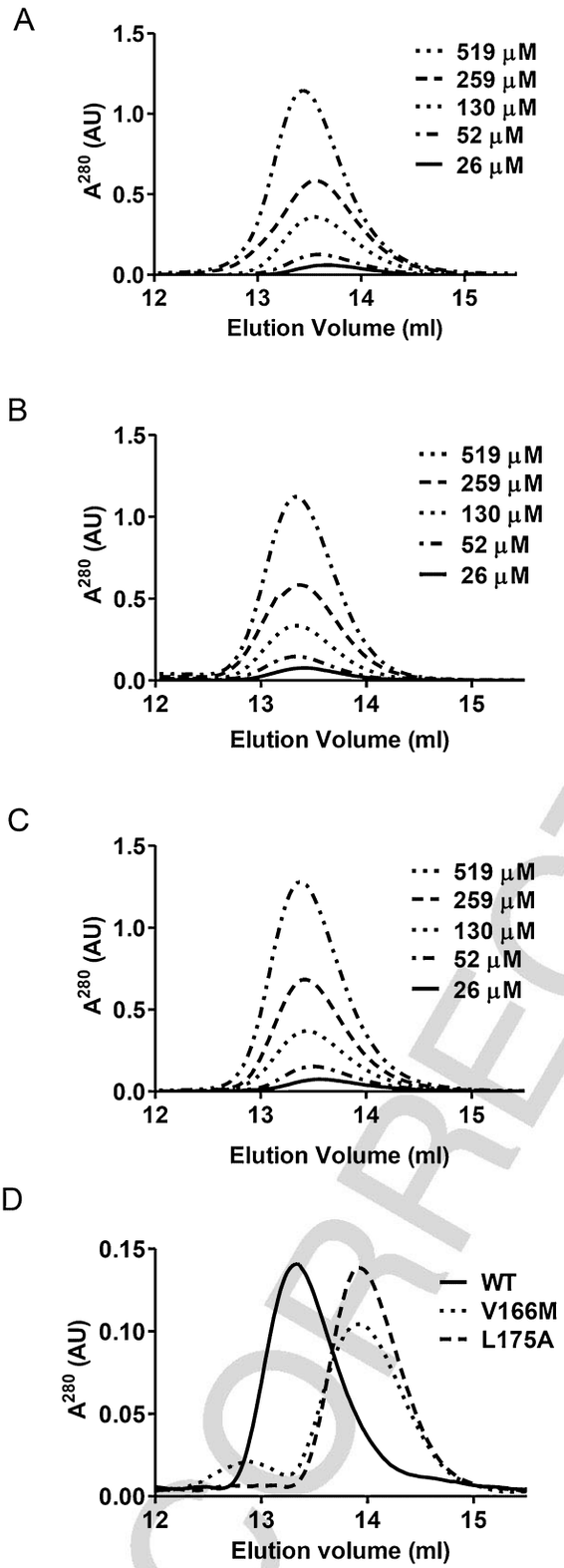

Fig. 4. Analysis of PAS2 dimerization by size exclusion chromatography. Concentration dependence of the elution profiles (when injected at five different concentrations as indicated in the legends) for (A) the wild-type PAS2 domain, (B) the 'redox signalling' variant I153A domain and (C) the 'redox signalling' variant F253L domain. (D) Elution profiles of the wild-type PAS2 domain (solid line) and the 'locked-on' variants V166M (dotted line) and L175A (dashed line) injected at a concentration of 104 μM. In all cases protein concentrations were calculated as the monomeric form. Elution volumes and the apparent molecular weights of each species are tabulated in the (Table S1).

26 μM, the retention volume remained constant with an apparent molecular weight of 39.6 kDa (Table S1). This may suggest that the I153A substitution shifts the monomer-dimer equilibrium towards the dimeric state. In contrast to the behaviour of wild-type PAS2 and the 'redox signalling' variants, the L175A substitution, which gives rise to a 'locked-on' phenotype in the full-length protein, eluted with an apparent molecular weight of 23.9 kDa (when injected at 104 μM), similar to that of the monomeric form (Fig. 4D, dashed line). The elution behaviour of L175A was also concentration-dependent but did not approach that of the dimeric form when injected at a higher concentration (Table S1). The $NifL_{(143–284)}$-V166M protein (104 μM) sieved as a mixture of two oligomeric species of 23.1 and 48.5 kDa (Fig. 4D, dotted line), which are likely to represent the monomeric and dimeric forms, respectively, of the mutant PAS2 domain. These data suggest that the monomer-dimer equilibrium is shifted towards the monomeric state in these 'locked-on' variants, conversant with the observation that these mutant PAS2 domains fail to interact in the bacterial two-hybrid system.

To further investigate the dynamic equilibrium between the monomeric and dimeric forms, we used analytical ultracentrifugation to analyse the sedimentation properties of the isolated PAS2 domain. Sedimentation equilibrium profiles of PAS2 revealed that the observed solution molecular mass varied between 24 and 35 kDa over a concentration range of 10–100 μM. In contrast, equilibrium profiles of the L175A form showed a variation of 22–28 kDa over a concentration range of 7–70 μM. Plotting the sedimentation equilibrium profiles in terms of log absorbance versus radius^2/2 is expected to give a straight line, where the gradient of the line is proportional to the molecular mass of the protein in solution (Horan *et al.*, 1995). The difference in apparent molecular mass of the two forms can be observed in Fig. 5, where the larger gradient of the data corresponding to the wild-type protein demonstrates a shift towards the dimeric species at the higher protein concentration (Fig. 5A), in contrast to the predominance of the monomeric form at the lower protein concentration (Fig. 5B). The sedimentation data for each species fitted best to a monomer-dimer model with a dissociation constant (K_d) of 34 μM for the wild type, and 120 μM for the L175A mutant; this reflects the difference

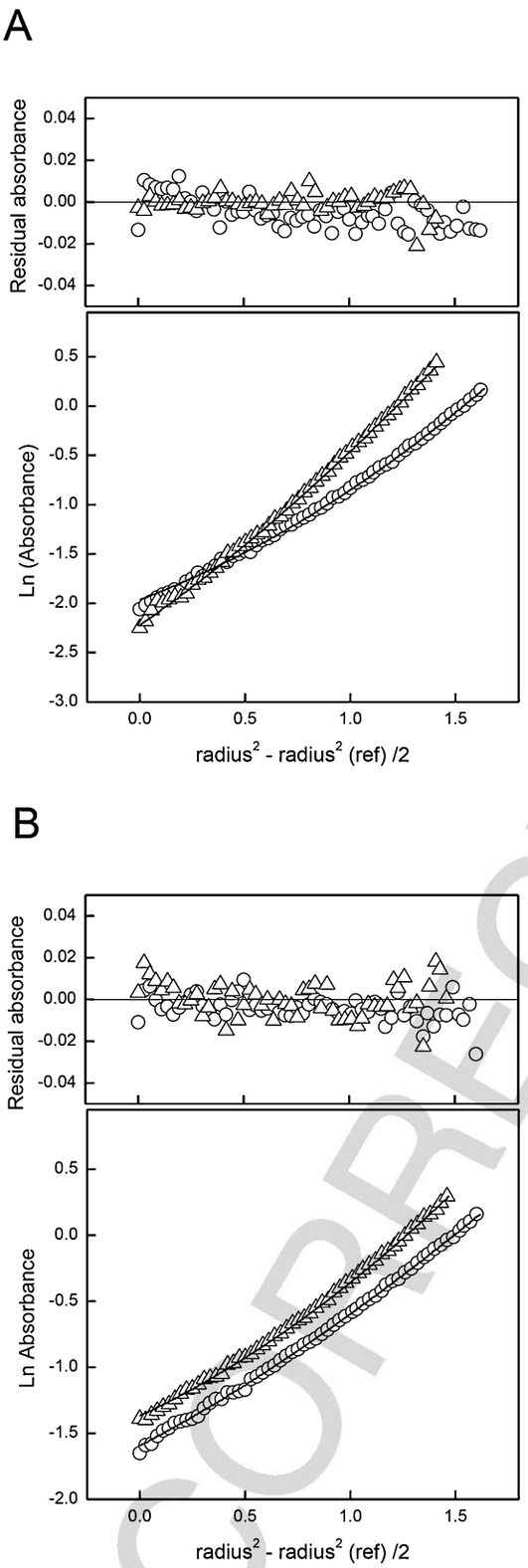

Fig. 5. Sedimentation equilibrium profiles of wild-type PAS2 (triangles) and L175A (circles) at a rotor speed of 23 000 r.p.m. Lower panels: (A) 100 μM PAS2 and 70 μM L175A measured at 275 nm, and (B) 10 μM PAS2 and 7 μM L175A measured at 230 nm. The lines represent a fit to both data sets for each sample using a 20 kDa monomer-dimer equilibrium model and K_d values of 34 and 120 μM for the wild type and L175A samples respectively. Upper panels: residual absorbance between the experimental data and the fitted lines.

between the two forms observed in both the sedimentation equilibrium and gel filtration experiments.

To further investigate subunit stoichiometry, the isolated PAS2 domain and its mutants were chemically cross-linked with glutaraldehyde and the products were analysed on SDS-PAGE (Fig. S1). These experiments indicated that the isolated PAS2 domain and all the variants tested can be cross-linked in the dimeric form and no cross-linked species corresponding to higher oligomers could be detected by SDS-PAGE. The 'locked-on' PAS2 variants exhibited a reduction in the percentage of cross-linked protein, suggesting a shift in the monomer-dimer equilibrium towards the monomeric form. In contrast, the F253L variant exhibited a similar level of cross-linked species to that of the wild-type PAS 2 domain, and the I153A mutant showed increased cross-linking relative to the wild type (Fig. S1), implying that this mutation may shift the equilibrium towards the dimeric state in agreement with the size exclusion analysis (Fig. 4). Overall, the results from the BACTH analysis, in combination with the chemical cross-linking, gel filtration chromatography and ultracentrifugation data, suggest that the 'locked-on' variants disrupt PAS2 dimerization while the 'redox signalling' variants do not.

PAS2 mutations do not influence the overall oligomerization state of NifL

Given that the 'locked-on' mutations apparently alter the quaternary structure of the isolated PAS2 domain, we questioned whether these mutations influence oligomerization of the full-length NifL protein. It was therefore important to establish whether the PAS2 domain is an oligomerization determinant of NifL or whether the oligomerization state of this domain is important for relaying structural signals between domains. Assessing this experimentally is complicated by the presence of two additional oligomerization interfaces in the NifL protein, as the PAS1 and H domains both contain dimerization surfaces. The crystal structure of NifL PAS1 is dimeric (Key *et al.*, 2007) and the H domain is predicted to form a coiled-coil structure homologous to the dimerization interface of the histidine protein kinases (Little *et al.*, 2007). Therefore, we analysed the oligomeric states of the 'locked-on' PAS2 mutants in the context of full length and

Table 3. Size exclusion chromatography of NifL domain combinations.

Protein construct	Domains present	Apparent Mw (kDa)	Expected monomeric Mw (kDa)	Apparent oligomerization state
NifL	PAS1, PAS2, H, GHKL	197.7	61.1	Trimer
NifL-V166M	PAS1, PAS2, H, GHKL	196.7	61.1	Trimer
$NifL_{(143–519)}$	PAS2, H, GHKL	108.1	45.3	Dimer
$NifL_{(143–519)}$-V166M	PAS2, H, GHKL	110.4	45.3	Dimer
$NifL_{(1–284)}$	PAS1, PAS2	96.3	35.0	Trimer
$NifL_{(1–284)}$-V166M	PAS1, PAS2	92.5	35.0	Trimer
$NifL_{(1–284)}$-I153A	PAS1, PAS2	92.8	35.0	Trimer

various truncated forms of NifL. These included a NifL construct containing only the two N-terminal PAS domains (lacking the H and GHKL domains) and one lacking only the PAS1 domain. The 'locked-on' substitution V166M had no effect on oligomerization in any of the constructs tested, when analysed by gel filtration chromatography (Table 3). $NifL_{(1–284)}$ (which contains only the two N-terminal PAS domains) sieved as a trimer on gel filtration with an apparent molecular mass of 96.3 kDa (Table 3).We believe that elution of this fragment on gel filtration columns may be aberrant, as in sedimentation velocity experiments this protein exhibits an average sedimentation coefficient of 3.17 S, equivalent to a dimer, irrespective of its redox state (data not shown). Sedimentation of this tandem PAS1-PAS2 fragment as a dimer was unexpected, given that we have previously shown that the isolated PAS1 domain behaves as a tetramer (Söderbäck *et al.*, 1998; and ••, unpubl. data). This discrepancy may imply that the presence of the PAS2 domain influences the oligomerization state of PAS1. Nevertheless, when introduced into the tandem PAS1-PAS2 fragment, the PAS2 substitutions I153A ('redox signalling' class) and V166M ('locked-on' class) did not influence the gel filtration elution profile when compared with the wild-type $NifL_{(1–284)}$ fragment (Table 3). Overall, these results suggest that the PAS2 dimerization interface, which is apparently disrupted by the 'locked-on' substitutions in the isolated PAS2 domain, does not influence the oligomerization state when combined with other NifL domains.

Bacterial two-hybrid analysis of fragments containing the two N-terminal PAS domains supported the results obtained from the gel filtration experiments. We detected self-association of the isolated PAS1 and PAS2 domains (Fig. 6, bars marked 'PAS1' and 'PAS2') as well as a longer construct in which both domains are present in tandem (Fig. 6, bars marked 'PAS1, PAS2'). As shown in Fig. 3, the 'locked-on' substitutions V157A and V166M disrupt oligomerization of the isolated PAS2 domain (Fig. 6, bars marked 'PAS2', 'PAS2-V157A' and 'PAS2-V166M'). However, when the PAS1 domain was also present, the effect of the 'locked-on' mutations on oligomerization was nullified and the mutant proteins showed the same level of interaction as the wild type in the two-hybrid system (Fig. 6, compare bars marked 'PAS1, PAS2', 'PAS1, PAS2-V157A' and 'PAS1, PAS2-V166M'). This demonstrates that the dimerization interface present in PAS1 (Key *et al.*, 2007; Ayers and Moffat, 2008) is sufficient to maintain oligomerization of the PAS1-PAS2 construct when PAS2 dimerization is impaired. The BACTH analysis was performed under oxygen-limiting conditions *in vivo*, unlike the gel filtration experiments, which were carried out under aerobic conditions. As the PAS1 domain was sufficient to maintain oligomerization of $NifL_{(1–284)}$ in both experiments, it appears that the oligomeric state of the PAS1-PAS2 construct is maintained irrespective of redox status. The PAS2 dimerization interface therefore is not important in maintaining the oligomeric state of NifL but instead seems to function in intramolecular signal transduction.

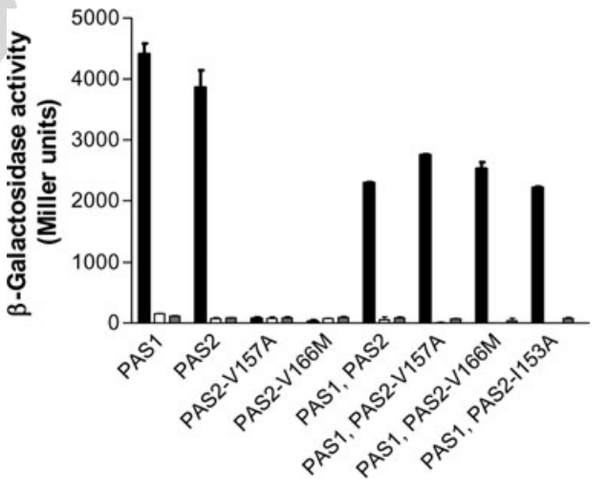

Fig. 6. BACTH analysis of the influence of PAS2 substitutions on oligomerization of the PAS1-PAS2 fragment of NifL. Hybrid proteins in which PAS1 (residues 1–146), PAS2 (residues 147–284) and PAS1-PAS2 (residues 1–284) fragments of NifL were fused to either subunit of adenylate cyclase and expressed as described in *Experimental Procedures*. The graph is presented as in Fig. 3 with interactions between two fusion proteins indicated by the black bars and controls shown as white or grey bars. Experiments were performed in duplicate and error bars indicate the standard error of the mean.

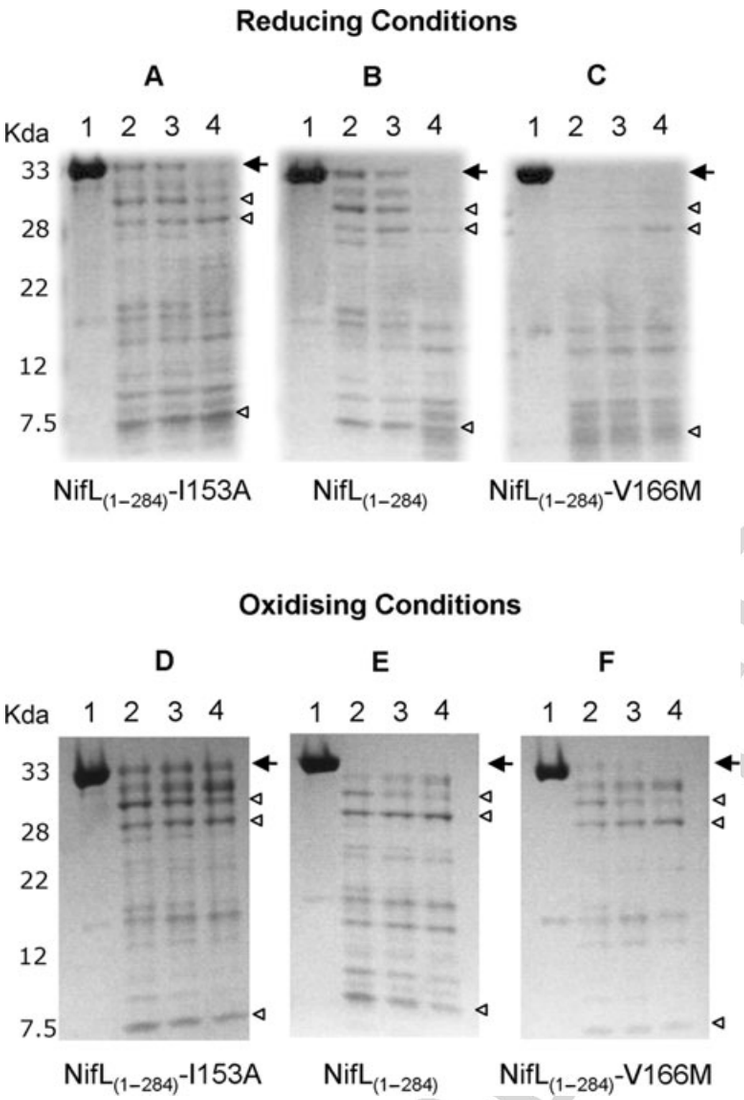

Fig. 7. Limited chymotrypsin proteolysis of the PAS1-PAS2 fragment of NifL. Proteins (final concentration 10 μM, calculated as a monomer) were incubated with chymotrypsin for 0, 2, 5 and 10 min (lanes 1, 2, 3 and 4, respectively, in each panel). Proteolysis experiments were performed on the wild-type PAS1-PAS2 fragment (B and E) and mutant fragments containing the 'locked-on' substitution V166M (C and F) or the 'redox signalling' substitution I153A (A and D) under either reducing conditions (A–C) or oxidizing conditions (D–F). The chymotrypsin : protein (w : w) ratio was 1:60. The full length (undigested fragment) in each case is indicated by the arrow. Approximate molecular weights determined by calibrations with markers are listed to the left of (A) and (D). Open arrowheads indicate putative proteolytic fragments arising from digestion at the chymotrypsin-sensitive sites F218 and F222 identified previously (Money *et al.*, 2001).

Redox-dependent conformational changes in the N-terminal PAS domains of NifL

The analysis of the variant proteins and domains presented thus far suggests that a large conformational change, involving a shift in the quaternary structure of the PAS2 domain, accompanies redox signal transduction in NifL. We wanted to investigate this conformational change in a wild-type context and check for congruence with the findings obtained using mutant proteins. To this end, limited chymotrypsin proteolysis was used to analyse the conformation of $NifL_{(1–284)}$ (a construct containing both the PAS1 and PAS2 domains) and its mutant forms under oxidizing and reducing conditions *in vitro* (Fig. 7). These experiments were carried out under anaerobic conditions in a glove box using sodium dithionite where appropriate to reduce the FAD cofactor in PAS1 (Hill *et al.*, 1996). Protein samples were incubated with chymotrypsin for time periods of 0, 2, 5 and 10 min (Fig. 7, lanes labelled 1, 2, 3 and 4 respectively) and the progress of the proteolysis reaction at each time point was analysed by SDS-PAGE.

When the FAD cofactor was reduced with sodium dithionite, the wild-type protein fragment, $NifL_{(1–284)}$, showed a similar rate and pattern of digestion to the 'redox signalling' variant $NifL_{(1–284)}$-I153A (Fig. 7, compare A and B). In both cases the undigested protein (indicated by the arrow) persisted after a 5 min incubation with protease (Fig. 7, compare lanes 3 of A and B) but was almost completely cleaved after 10 min incubation (Fig. 7, lanes 4 in A and B). In contrast, a different proteolysis pattern was observed with $NifL_{(1–284)}$-V166M, which was largely digested within 2 min of exposure to chymotrypsin (Fig. 7C). This suggests that under reducing conditions,

NifL$_{(1–284)}$ adopts a similar conformation to that of NifL$_{(1–284)}$-I153A, while differing in conformation to NifL$_{(1–284)}$-V166M. However, when the FAD cofactor was oxidized, there was a change in the proteolytic footprint of NifL$_{(1–284)}$. In contrast to the digestion pattern observed under reducing conditions, the footprint of the oxidized NifL$_{(1–284)}$ construct closely resembled that of NifL$_{(1–284)}$-V166M (Fig. 7, compare E and F). In both cases, the band corresponding to full-length protein was digested within 2 min of addition of the protease. This shift in the proteolysis pattern of wild-type NifL$_{(1–284)}$ implies a redox-dependent change in protein conformation (Fig. 7, compare B and E). Moreover, the proteolytic footprint of NifL$_{(1–284)}$ resembles that of the 'redox signalling' variant under reducing conditions and that of the 'locked-on' mutant protein under oxidizing conditions. To eliminate the possibility that the PAS2 mutations influence the incorporation of FAD into PAS1, the FAD content of all constructs was determined and no significant differences were observed (data not shown). As an additional control, the oxidation state of the FAD group was monitored spectroscopically to check that the dithionite concentration used was sufficient to fully reduce the moiety in all of the protein constructs (data not shown). Overall, it seems that oxidation reduction of the FAD group in PAS1 triggers a shift between two distinct conformations of the PAS1-PAS2 construct and that the mutations in the PAS2 domain cause the protein to favour one of these conformers over the other (regardless of signal perception by the PAS1 domain). It is also worth noting that the rate of digestion of NifL$_{(1–284)}$ was faster under oxidizing conditions than under reducing conditions (Fig. 7B and E). This is consistent with the hypothesis that PAS2 subunits dissociate in response to oxidation of the PAS1 cofactor leading to a more open conformation.

Discussion

The data presented here demonstrate that the PAS2 domain of NifL can exist in two discrete states, as exemplified by mutations that stabilize NifL in either the 'on' or the 'off' conformation. The 'on' mutations in PAS2 result in a form of NifL that is competent to inhibit NifA, irrespective of the redox state of the FAD cofactor in the PAS1 domain. Our limited proteolysis experiments suggest that these mutations lock NifL in a conformation similar to that of the oxidized form. This may explain why these variants exhibit diminished responses to nitrogen availability because oxidation of the FAD group results in a conformation of NifL that overrides control by fixed nitrogen (Söderbäck *et al.*, 1998). In contrast, the 'off' mutations in PAS2 apparently fail to communicate the redox state of PAS1 to the C-terminal domains of NifL, but the variant proteins remain responsive to the fixed nitrogen signal conveyed by interaction with the signal transduction protein, GlnK (Little *et al.*, 2002; Rudnick *et al.*, 2002). 'Off' mutations might influence redox signal transduction in NifL by several different mechanisms including: (i) disrupting interactions between the PAS1 and PAS2 domains, (ii) perturbing interactions between PAS2 and the C-terminal domains of NifL or (iii) stabilizing the reduced conformation relative to the oxidized conformer. Whatever the mechanism, our combined results directly demonstrate an important role for PAS2 in redox signal relay from PAS1 to influence the interaction of the C-terminal domains with NifA.

The quaternary arrangement of the PAS2 subunits within NifL is apparently an important component in redox signal transduction. Whereas the isolated PAS2 domain is a dimer in solution and the 'off' state variants are also dimeric, all of the 'on' state mutations we have analysed appear to influence the association state of the isolated PAS2 domain towards the monomeric form. However, these changes in association state are not apparent when PAS2 is combined with other domains, suggesting that PAS2 does not contribute to oligomerization of NifL, but rather provides an interface for alternative quaternary arrangements. It is noteworthy that most of the 'on' mutants we have identified are apparently located within the proposed extended dimerization interface identified recently in PAS domain structures. In addition to the conserved dimerization motif represented by the N-terminal A′α helix (Key *et al.*, 2007; Ma *et al.*, 2008) structure-based alignments have identified a number of conserved residues in the dimer interface located on the β strands (Ayers and Moffat, 2008). Although no structural data are available for the NifL PAS2 domain, V166, L175 and L262 are likely to correspond to residues in the conserved β sheet interface and V157 is predicted to be positioned within the N-terminal α helix (Fig. 1).

Our results suggest a model of signal transduction in NifL whereby changes in the quaternary structure of the PAS2 domain mediate the transmission of redox signals from the PAS1 domain to the C-terminal domains of NifL (Fig. 8). In this model, oxidation of the FAD cofactor induces a conformational change in the PAS1 domain that is communicated to the PAS2 domain, triggering a shift in the monomer-dimer equilibrium to favour the dissociation of PAS2 subunits. This movement of the PAS2 protomers is likely to generate re-organization of the H and GHKL domains of NifL to promote binding of NifL to NifA.

The PAS domains have been shown to undergo signal-dependent conformational changes particularly in the C-terminal beta sheet regions (Erbel *et al.*, 2003; Card *et al.*, 2005; Evans *et al.*, 2009) that may provoke alterations in quaternary structure. The *Bacillus subtilis* YtvA protein provides a well-studied example of a PAS domain that exhibits a stimulus-dependent quaternary structural

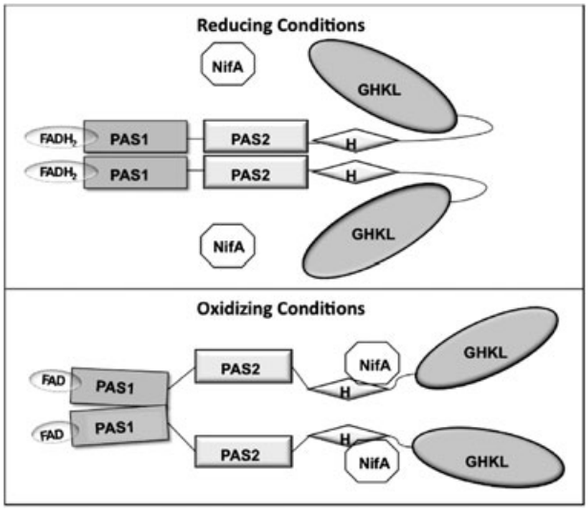

Fig. 8. Model of redox signal transduction in NifL. Under reducing conditions when FAD cofactor is fully protonated, the PAS2 domain is maintained in the dimeric state and the H and GHKL domains are in a conformation that prevents NifA from accessing the surfaces of NifL that mediate the interaction with NifA. Under these conditions, NifA escapes inhibition by NifL. Oxidation of the FAD cofactor generates a conformational change in the PAS1 domain, which is communicated to the PAS2 domain, triggering a movement of PAS2 protomers. This shift in the quaternary structural arrangement of the PAS2 domain results in a re-organization of the H and GHKL domains of NifL to promote inhibition of NifA activity.

change. YtvA regulates responses to blue-light illumination and contains an N-terminal PAS domain that binds an FMN cofactor. This domain forms a stable dimer and the subunits of the PAS dimer rotate by 4–5° relative to one another in response to blue light illumination (Möglich and Moffat, 2007). Similarly, oxidation of the haeme iron in the dimeric PAS-A domain from *E. coli* Dos (EcDos) leads to a 3° rotation of the subunits with respect to each other (Kurokawa *et al.*, 2004) and ligand binding to the haeme cofactor in the *bj*FixLH dimer results in a ~2° rotation of the subunits (Ayers and Moffat, 2008). A similar rotation may enable the subunits of NifL PAS1 to undergo a 'scissor-like' movement with respect to one another in response to redox changes, to influence in turn the quaternary structure of PAS2 (Fig. 8). As redox signal transduction by PAS1 appears to alter the oligomerization state of PAS2, resulting in dissociation of the dimer under oxidizing conditions, it is possible that this provides a mechanism for amplifying the signal to effect the conformational movements necessary to switch the activity of the C-terminal domains of NifL. The importance of the monomer-dimer equilibrium in signal relay by the PAS2 domain mirrors the properties of other PAS domains in which homo- or heterodimerization plays an important role in the signalling mechanism, for example, the light-sensing proteins Vivid and phototropin (Zoltowski *et al.*, 2007; Nakasone *et al.*, 2008), and the *B. subtilis* KinA protein (Lee *et al.*, 2008).

The properties of NifL PAS2 suggest that it is a representative of an emerging subclass of PAS domains that are apparently involved in signal relay rather than sensing. The presence of multiple PAS domains within a single protein is surprisingly common; according to the SMART nrdb database there are a total of 22 276 PAS domains found in 14597 proteins (http://smart.embl.de/smart/do_annotation.pl?DOMAIN=PAS 04/10/2009). Of the relatively few PAS domains characterized to date, it is often the case that no obvious sensory function can be attributed to the additional PAS domain(s) within a tandem pair (or triplet). There are several examples of well-studied PAS domains that may belong to this subclass. DcuS is a membrane-embedded histidine kinase that contains a periplasmic C4-dicarboxylate-sensing PAS domain (PASp), which transmits signals to a cytoplasmic PAS domain (PASc) via two transmembrane helices. The PASc domain has no known role in signal perception, but the plasticity of this domain is believed to be important for signal transduction to the histidine kinase domains. When substitutions in PASc resulting in ligand-independent (constitutive) activation of DcuS were modelled on the dimeric crystal structure of NifL PAS1, it was observed that these residues were located close to the α-helical N-terminal cap that forms part of the dimerization interface (Etzkorn *et al.*, 2008). This suggests a model in which signal perception by DcuS PASp impacts upon the stability of the dimer interface in DcuS PASc, analogous to the influence of NifL PAS1 on the quaternary structure of NifL PAS2. Another example of the potential role of PAS domains in signal relay is provided by KinA, a cytoplasmic histidine kinase that regulates sporulation in *B. subtilis* in response to unknown signal(s). KinA has an N-terminal sensory region that consists of three PAS domains. The oligomerization state of the most N-terminal of these PAS domains, PAS-A, is important for histidine kinase function. Substitutions that favour the monomeric state of the isolated PAS-A domain activate autokinase activity in the full-length KinA protein (Lee *et al.*, 2008). Intriguingly, structural predictions indicate that the substitution in PAS-A giving rise to the greatest level of kinase activity, Y29A, is found at a position equivalent to L175 in NifL PAS2 (Fig. 1). Both Y29A and L175A strongly disrupt dimerization of their respective PAS domains. Further analogies can be drawn between the sensory regions of KinA and NifL in that both contain duplicate PAS domains that have no known role in signal perception yet can influence the conformation of downstream domains via changes in quaternary structure. Other examples of this class may include the redox sensing region of MmoS, which like NifL contains an N-terminal FAD-binding sensory PAS domain and a more C-terminal PAS domain

of unknown function (Ukaegbu and Rosenzweig, 2009) and EcDos, which contains an N-terminal haeme containing PAS domain in tandem with a second PAS domain (Sasakura *et al*., 2006).

Our data demonstrate that within NifL, the two PAS domains function in tandem and the quaternary structure of PAS2 is responsive to signal perception by PAS1. In addition, mutations in NifL PAS2 are sufficient to either block the relay of signals from PAS1 or mimic the active state in the absence of a signal. For cytoplasmic proteins, the benefits of having an additional PAS domain solely for signal relay are not readily apparent. In the examples discussed above multiple PAS domains might be advantageous for amplification of structural signals, thus driving appropriate conformational changes in the C-terminal HisKA (or H in the case of NifL) and GHKL domains. Current models for histidine kinase autophosphorylation and phosphotransfer, based on crystal structures suggest that large movements of the HisKA and GHKL domains relative to one another are required for signalling (Marina *et al*., 2005; Albanesi *et al*., 2009; Casino *et al*., 2009). However, not all histidine kinases have multiple PAS domains and, for example, experiments with chimeric proteins demonstrate that the single light-sensing PAS domain from YtvA is sufficient to provide input signal specificity and regulate the activity of the C-terminal kinase domains of FixL in response to light (Möglich and Moffat, 2007). Both YtvA and FixL contain an α-helical coiled-coil linker, connecting their input and output domains, comprising the Jα helix often found associated with PAS domains. Signal-dependent unfolding of this coiled-coil sequence may result in rotational movements that regulate kinase activity (Harper *et al*., 2003; 2004; Möglich and Moffat, 2007; Möglich *et al*., 2009). In proteins such as NifL, DcuS and KinA it is possible that this α-helical coiled-coil mechanism is replaced by the 'signal relay' PAS domain, which provides conformational flexibility associated with the interconversion between the dimeric and monomeric forms. As many histidine kinases contain multiple PAS domains of unknown function, we cannot eliminate the possibility that some of these additional PAS domains respond to as yet undiscovered stimuli and can modulate signal relay accordingly. In other words, there is potential for some 'signal relay' PAS domains to act as biological 'logic gates' to aid the integration of multiple signals within a single protein.

Experimental procedures

Site-directed mutagenesis

All site-directed mutations were constructed using a two-step PCR technique. The first step consisted of two PCR reactions: one carried out with the forward primer L1x (5′-CCGCCGCAAGGACAAGACC-3′) and a reverse primer containing the desired mutation and the other with the reverse primer Nic1 (5′-GATCATGCTGCGCAGGC-TGCTTTC-3′) and a forward primer containing the desired mutation. The products of these first step PCR reactions were purified (Qiagen kit) and used as template DNA for the second-step PCR reaction using the above primers L1x and Nic1. The resulting fragments were purified (Qiagen kit) and cut with the restriction enzymes MluI and ApaI. The digested fragment was then cloned into pPR34. All mutations were confirmed by DNA sequencing.

Random mutagenesis

The PCR mutagenesis was carried out with *Taq* DNA polymerase (Roche) under standard reaction conditions. Reaction mixtures contained 75 ng of template pPR34, 100 ng of each primer (primers L1x and Nic1 were used), 0.2 mM dNTPs, 1.5 mM $MgCl_2$ and 5 units of enzyme in a final volume of 50 µl. The PCR products were purified (Qiagen kit) and cut with restriction endonucleases MluI and ApaI and subsequently recloned (after gel purification using a Qiagen kit) into pPR34 cut with the same enzymes. Ligation mixtures were then cycled through *E. coli* strain DH5α to amplify the DNA content. The resultant plasmids (containing the PCR-generated insert) were transformed into *E. coli* strain ET8000, which contains the reporter plasmid pRT22 (carrying a *nifH–lacZ* fusion). Transformants were screened on NFDM medium supplemented with casein hydroxylate (200 µg ml^{-1}), Xgal (5-bromo-4chloro-3-indolyl-B-D-galactopyranoside, 40 µg ml^{-1}), Chloramphenicol (30 µg ml^{-1}) and Carbenicillin (100 µg ml^{-1}). NifL mutants resulting in altered NifA activity were selected (see *Results*) and their plasmid DNA recovered and sequenced to identify mutations. Plasmids of known sequence were then transformed back into the host strain for further phenotypic analysis.

β-Galactosidase assays

Growth conditions and β-galactosidase assays to determine NifA activity were performed as described previously (Perry *et al*., 2005; Little *et al*., 2007). β-Galactosidase assays for BACTH analysis were carried out according to the same procedure, except that cultures were grown in sealed plastic vials (internal volume 7 ml) at 30°C in LB medium supplemented with 1% glucose, 0.5 mM IPTG (isopropyl-β-*D*-thiogalactopyranoside) and appropriate antibiotics.

Plasmid construction

Plasmids pPS54 and pPS77 (encoding $NifL_{(143–519)}$ and $NifL_{(143–519)}$-V166M, respectively, cotranscribed with NifA from a constitutive promoter) were created by PCR amplification of the *nifL* gene from plasmid pPR34 (Söderbäck *et al*., 1998) and a derivative plasmid, pPS20, encoding the V166M substitution. The forward primer pPS54a (5′-GCGAA TTGCACCATATGGAACAACGC-3′) was used to introduce an NdeI site immediately prior to the DNA sequence encoding residue 143 and the reverse primer used was Nic 1 (5′-GATCATGCTGCGCAGGCTGCTTTC-3). The PCR product was then digested with NdeI and NotI and re-cloned into

pPR34 (or pPS20) that had been digested with the same enzymes. Plasmid pPS124 (encoding NifL-V166M, G480A cotranscribed with NifA) was constructed by digesting pPS20 with the restriction endonucleases NdeI and NotI, gel purifying the resultant *nifL* fragment (Qiagen kit) and cloning this into plasmid pNLG480A (Perry *et al*., 2005) digested with the same enzymes. All constructs were confirmed by DNA sequencing.

Western blotting

To obtain protein extracts, cultures of ET8000 cells containing the plasmid of interest were grown as for the β-galactosidase assays. To ensure that cell numbers were equivalent between samples, the volume taken from each culture was adjusted according to differences in OD_{600}. The normalized cell samples were then centrifuged and the pellet resuspended in protein loading buffer (125 mM Tris-HCl, 4% sodium dodecyl sulphate, 20% glycerol, 10% β-mercaptoethanol, 0.05% bromophenol blue, pH 6.8). The proteins were then separated by SDS-PAGE and electrotransfered onto nitrocellulose membranes. Membranes were probed with polyclonal antisera against NifL and primary antibodies were detected with alkaline phosphatize-conjugated anti-rabbit secondary antibodies. Secondary antibodies were detected by staining with 5-bromo-4-chloro-3-indolylphosphate and nitroblue tetrazolium.

BACTH analysis

DNA fragments encoding the protein of interest flanked by a 5′ BamHI site and a-3′ KpnI site (immediately preceded by a stop codon) were generated by PCR. Primers NifL-BTH-F (5′-GAGGATCCCARGACCCCGGCCAACCCGAC-3′) and PAS2-BTH-2R (5′-CTTAGGTACCTTCAGCGCGTTGAG-3′) were used to amplify the region of *nifL* encoding amino acids 1–284. The forward primer NifL-PAS-BTH-1F (5′-GAGGATCCCAACAACCAGCGCCTG-3′) and the reverse primer mentioned above, PAS2-BTH-2R, were used to generate DNA fragments encoding residues 143–284 of the NifL protein. Plasmid pPR34 or derivative plasmids containing the desired mutation were used as template DNA. PCR products were purified (Qiagen kit), digested with KpnI and BamHI, and cloned into the BACTH vectors pT25 and pUT18. All constructs were confirmed by DNA sequencing. The plasmids pT25 and pUT18, or derivatives containing the desired NifL sequence, were then cotransformed into chemically competent BTH101 cells (F′, *cya*-99, *ara*D139, *gal*E15, *gal*K16, *rps*L1(StrR), *hsd*R2, *mcr*A1, *mcr*B1; (Karimova *et al*., 2000) and plated onto LB medium supplemented with Xgal (40 μg ml^{-1}), chloramphenicol (30 μg ml^{-1}), carbenicillin (100 μg ml^{-1}) and IPTG (0.5 mM). Agar plates were incubated at 30°C for 72 h and checked for homology before a colony was picked and assayed for β-galactosidase activity as described above.

Plasmids for overexpression and protein purification

To construct plasmids for overexpression of $N_{his6}NifL_{(143–284)}$, $N_{his6}NifL_{(1–284)}$ and mutant derivatives, DNA fragments encoding the appropriate NifL residues flanked by a 5′ NcoI site and a 3′ BamHI site were generated by PCR using the forward primers Nco1-E143-NifL (5′-CAAGCGCCATGGAACAACGC GTCAACAACC-3′) or NifLNcoFor (5′-CGCATCCATGGCC ACCCCGGCCAACCCGACCCT-3′) and the reverse primer NifL-284-TGA-Bam (5′-GCAAGGATCCTCACTTCAGCGCG TTGAGCCG-3′). Plasmid pPR34 or derivatives from mutagenesis (see above) were used as template DNA. The NcoI-BamHI digested fragments were then cloned into the plasmid pETM-11 (EMBL). Constructs for overexpression of $N_{his6}NifL_{(143–519)}$, $N_{his6}NifL$ and mutant variants were derived from fragments encoding the appropriate NifL residues flanked by a 5′ NdeI site and a 3′ BamHI site, which were PCR-amplified from pPR34 (for $N_{his6}NifL$), pPS54 (for $N_{his6}NifL_{(143–519)}$, see *plasmid construction*) or mutant derivatives. The forward primer Pa1 (5′-CTAGAGAAT TCGGATAGACGAGGCACC-3′) and the reverse primer NifL2 (5′-CGAAGGATCCTCAGGTGGAGGCCGAGAAGGG-3′) were used in the PCR reaction and the products were then digested with the restriction endonucleases NdeI and BamHI. The resultant DNA fragment was cloned into a plasmid derived from pETM-11 (called pETNdeM-11) in which the NcoI site in the multiple cloning region was mutated to yield a NdeI site via a two-step PCR mutagenesis technique similar to that described above. All constructs were confirmed by DNA sequencing. In all cases overexpression was carried out in BL21(DE3)pLysS. Cultures were grown aerobically in Luria–Bertani broth and expression from the T7 promoter was induced by the addition of IPTG to a final concentration of 1 mM. Proteins were purified as described previously (Reyes-Ramirez *et al*., 2002; Little and Dixon, 2003; Little *et al*., 2007).

Gel filtration chromatography

Gel filtration chromatography was performed over a Superose 12 10/300 GL column (GE healthcare) equilibrated with 50 mM Tris-HCl, pH 8.0, 100 mM NaCl and 5% glycerol. Proteins were injected at a concentration of 104 μM (calculated as a monomer) unless otherwise stated. Bio-Rad gel filtration standards [thyroglobulin (bovine), γ-globulin (bovine), ovalbumin (chicken), myoglobin (horse) and vitamin B12] were used for calibration.

Analytical ultracentrifugation

Sedimentation equilibrium experiments were performed in a Beckman Optima XL-I analytical ultracentrifuge equipped with absorbance optics and an An50Ti rotor. The PAS2 domain ($N_{his6}NifL_{143–284}$) was diluted to concentrations of 10 and 100 μM while the L175A form was diluted to 7 and 70 μM (calculated as a monomer). Both forms were prepared in a final buffer concentration of 50 mM KH_2PO_4 (pH 8.0), 100 mM NaCl. One hundred and then microlitres of each sample was loaded into the sample sector of charcoal-filled Epon double sector cells fitted with quartz windows, while 120 μl of buffer was loaded into the reference sector. Samples were centrifuged at speeds of 16 000 and 23 000 r.p.m. and the absorbance was recorded at 275 nm for concentration of 70 and 100 μM protein, and 230 nm for protein concentrations of 7 and 10 μM. Data analysis was executed using Ultrascan II

(Demeler, 2005) where profiles of individual samples were initially analysed at single speeds using an ideal, single-component model. The parameters for buffer density and partial specific volume were determined using SEDNTERP (Horan *et al*., 1995). In order to best describe the sedimentation profiles for each PAS2 form, it was necessary to use a monomer-dimer equilibrium model to fit both concentration and rotor speeds simultaneously.

Limited chymotrypsin proteolysis

Chymotrypsin proteolysis was performed in TA buffer (50 mM Tris acetate, pH 7.0, 100 mM potassium acetate, 1 mM dithiothreitol) at 25°C. Samples were incubated for 1 h before initiating digestion with α-chymotrypsin (sigma, from bovine pancreas). The protease was diluted from a 0.5 mg ml^{-1} stock solution to a final chymotrypsin : $NifL_{(1–284)}$ weight ratio of 1:60 and $NifL_{(1–284)}$ was diluted from a 100 μM (based on a monomer) stock solution to a final concentration of 10 μM. The total reaction volume was 120 μl. At the times indicated in Fig. 6 and 15 μl of the sample was withdrawn and added to microcentrifuge tubes containing 0.35 μg of chymotrypsin inhibitor (Roche). An equal volume of gel loading buffer (Expedeon 4× sample buffer) was added and samples were heated to 70°C for 10 min before separation by SDS-PAGE on 12% polyacrylamide gels. For reducing conditions, all samples and stock solutions were prepared in sealed glass bijou tubes and sparged with oxygen-free nitrogen for 3 min before being transferred to a Belle anaerobic chamber (in which the oxygen level was maintained below 3.5 p.p.m.). The stock solution of $NifL_{(1–284)}$ was reduced with a 100-fold excess of dithionite (5 mM) and a sample removed for spectroscopic analysis to confirm that the flavin cofactor was fully reduced. The proteolysis experiment was then performed as described above.

Acknowledgements

We thank the Biotechnology and Biological Sciences Research Council for support and the award of a Doctoral Training Grant to P.S. Paloma Salinas was supported by a fellowship from the Conselleria d'Empresa, Universitat i Ciència, Generalitet Valenciana, Spain.

References

Albanesi, D., Martin, M., Trajtenberg, F., Mansilla, M.C., Haouz, A., Alzari, P.M., *et al.* (2009) Structural plasticity and catalysis regulation of a thermosensor histidine kinase. *Proc Natl Acad Sci* **106:** 16185–16190.

Ayers, R.A., and Moffat, K. (2008) Changes in quaternary structure in the signaling mechanisms of PAS domains. *Biochemistry* **47:** 12078–12086.

Card, P.B., Erbel, P.J.A., and Gardner, K.H. (2005) Structural basis of ARNT PAS-B dimerization: use of a common beta–sheet interface for hetero- and homodimerization. *J Mol Biol* **353:** 664–677.

Casino, P., Rubio, V., and Marina, A. (2009) Structural insight into partner specificity and phosphoryl transfer in two-component signal transduction. *Cell* **139:** 325–336.

Demeler, B. (2005) ••. In *Analytical Ultracentrifugation.* Scott, D., Harding, S., and Rowe, A. (eds). Cambridge: RCS, pp. 210–229.

Dixon, R., and Kahn, D. (2004) Genetic regulation of biological nitrogen fixation. *Nat Rev Microbiol* **2:** 621–631.

Erbel, P.J.A., Card, P.B., Karakuzu, O., Bruick, R.K., and Gardner, K.H. (2003) Structural basis for PAS domain heterodimerization in the basic helix-loop-helix-PAS transcription factor hypoxia-inducible factor. *Proc Natl Acad Sci USA* **100:** 15504–15509.

Etzkorn, M., Kneuper, H., Dunnwald, P., Vijayan, V., Kramer, J., Griesinger, C., *et al.* (2008) Plasticity of the PAS domain and a potential role for signal transduction in the histidine kinase DcuS. *Nat Struct Mol Biol* **15:** 1031–1039.

Evans, M.R., Card, P.B., and Gardner, K.H. (2009) ARNT PAS-B has a fragile native state structure with an alternative β-sheet register nearby in sequence space. *Proc Natl Acad Sci USA* **106:** 2617–2622.

Eydmann, T., Söderbäck, E., Jones, T., Hill, S., Austin, S., and Dixon, R. (1995) Transcriptional activation of the nitrogenase promoter *in vitro*: adenosine nucleosides are required for inhibition of NIFA activity by NIFL. *J Bacteriol* **177:** 1186–1195.

Harper, S.M., Neil, L.C., and Gardner, K.H. (2003) Structural basis of a phototropin light switch. *Science* **301:** 1541–1544.

Harper, S.M., Christie, J.M., and Gardner, K.H. (2004) Disruption of the LOV–Jalpha helix interaction activates phototropin kinase activity. *Biochemistry* **43:** 16184–16192.

Hill, S., Austin, S., Eydmann, T., Jones, T., and Dixon, R. (1996) *Azotobacter vinelandii* NIFL is a flavoprotein that modulates transcriptional activation of nitrogen-fixation genes via a redox-sensitive switch. *Proc Natl Acad Sci USA* **93:** 2143–2148.

Horan, T., Wen, J., Arakawa, T., Liu, N., Brankow, D., Hu, S., *et al.* (1995) Binding of neu differentiation factor with the extracellular domain of Her2 and Her3. *J Biol Chem* **270:** 24604–24608.

Karimova, G., Pidoux, J., Ullmann, A., and Ladant, D. (1998) A bacterial two-hybrid system based on a reconstituted signal transduction pathway. *Proc Natl Acad Sci USA* **95:** 5752–5756.

Karimova, G., Ullmann, A., and Ladant, D. (2000) A bacterial two-hybrid system that exploits a cAMP signaling cascade in Escherichia coli. *Methods Enzymol* **328:** 59–73.

Key, J., Hefti, M., Purcell, E.B., and Moffat, K. (2007) Structure of the redox sensor domain of *Azotobacter vinelandii* NifL at atomic resolution: signaling, dimerization, and mechanism. *Biochemistry* **46:** 3614–3623.

Kurokawa, H., Lee, D.-S., Watanabe, M., Sagami, I., Mikami, B., Raman, C.S., and Shimizu, T. (2004) A Redox-controlled molecular switch revealed by the crystal structure of a bacterial heme PAS sensor. *J Biol Chem* **279:** 20186–20193.

Lee, J., Tomchick, D.R., Brautigam, C.A., Machius, M., Kort, R., Hellingwerf, K.J., and Gardner, K.H. (2008) Changes at the kinA PAS-A dimerization interface influence histidine kinase function. *Biochemistry* **47:** 4051–4064.

Little, R., and Dixon, R. (2003) The amino-terminal GAF domain of *Azotobacter vinelandii* NifA binds 2-oxoglutarate to resist inhibition by NifL under nitrogen-limiting conditions. *J Biol Chem* **278:** 28711–28718.

Little, R., Reyes-Ramirez, F., Zhang, Y., van Heeswijk, W.C., and Dixon, R. (2000) Signal transduction to the *Azotobacter vinelandii* NIFL-NIFA regulatory system is influenced directly by interaction with 2-oxoglutarate and the PII regulatory protein. *EMBO J* **19:** 6041–6050.

Little, R., Colombo, V., Leech, A., and Dixon, R. (2002) Direct interaction of the NifL regulatory protein with the GlnK signal transducer enables the *Azotobacter vinelandii* NifL-NifA regulatory system to respond to conditions replete for nitrogen. *J Biol Chem* **277:** 15472–15481.

Little, R., Martinez-Argudo, I., Perry, S., and Dixon, R. (2007) Role of the H domain of the histidine kinase-like protein NifL in signal transmission. *J Biol Chem* **282:** 13429–13437.

Ma, X., Sayed, N., Baskaran, P., Beuve, A., and van den Akker, F. (2008) PAS-mediated dimerization of soluble guanylyl cyclase revealed by signal transduction histidine kinase domain crystal structure. *J Biol Chem* **283:** 1167–1178.

Macheroux, P., Hill, S., Austin, S., Eydmann, T., Jones, T., Kim, S.-O., *et al.* (1998) Electron donation to the flavoprotein NifL, a redox-sensing transcriptional regulator. *Biochem J* **332:** 413–419.

Marina, A., Waldburger, C.D., and Hendrickson, W.A. (2005) Structure of the entire cytoplasmic portion of a sensor histidine-kinase protein. *EMBO J* **24:** 4247–4259.

Martinez-Argudo, I., Little, R., Shearer, N., Johnson, P., and Dixon, R. (2004a) The NifL-NifA system: a multidomain transcriptional regulatory complex that integrates environmental signals. *J Bacteriol* **186:** 601–610.

Martinez-Argudo, I., Little, R., and Dixon, R. (2004b) A crucial arginine residue is required for a conformational switch in NifL to regulate nitrogen fixation in *Azotobacter vinelandii*. *Proc Natl Acad Sci USA* **101:** 16316–16321.

Martinez-Argudo, I., Little, R., and Dixon, R. (2004c) Role of the amino-terminal GAF domain of the NifA activator in controlling the response to the anti-activator protein NifL. *Mol Microbiol* **52:** 1731–1744.

Möglich, A., Ayers, R.A., and Moffat, K. (2009) Design and signaling mechanism of light-regulated histidine kinases. *J Mol Biol* **385:** 1433–1444.

Möglich, A., and Moffat, K. (2007) Structural basis for light-dependent signaling in the dimeric lov domain of the photosensor YtvA. *J Mol Biol* **373:** 112–126.

Money, T., Barrett, J., Dixon, R., and Austin, S. (2001) Protein–protein interactions in the complex between the enhancer binding protein NIFA and the sensor NIFL from *Azotobacter vinelandii*. *J Bacteriol* **183:** 1359–1368.

Money, T., Jones, T., Dixon, R., and Austin, S. (1999) Isolation and properties of the complex between the enhancer binding protein NIFA and the sensor NIFL. *J Bacteriol* **181:** 4461–4468.

Nakasone, Y., Eitoku, T., Zikihara, K., Matsuoka, D., Tokutomi, S., and Terazima, M. (2008) Stability of dimer and domain–domain interaction of arabidopsis phototropin 1 LOV2. *J Mol Biol* **383:** 904–913.

Perry, S., Shearer, N., Little, R., and Dixon, R. (2005) Mutational analysis of the nucleotide-binding domain of the anti-activator NifL. *J Mol Biol* **346:** 935–949.

Reyes-Ramirez, F., Little, R., and Dixon, R. (2001) Role of *Escherichia coli* nitrogen regulatory genes in the nitrogen response of the *Azotobacter vinelandii* NifL-NifA complex. *J Bacteriol* **183:** 3076–3082.

Reyes-Ramirez, F., Little, R., and Dixon, R. (2002) Mutant forms of the *Azotobacter vinelandii* transcriptional activator NifA resistant to inhibition by the NifL regulatory protein. *J Bacteriol* **184:** 6777–6785.

Rudnick, P., Kunz, C., Gunatilaka, M.K., Hines, E.R., and Kennedy, C. (2002) Role of GlnK in NifL-mediated regulation of NifA activity in *Azotobacter vinelandii*. *J Bacteriol* **184:** 812–820.

Sasakura, Y., Yoshimura-Suzuki, T., Kurokawa, H., and Shimizu, T. (2006) Structure-function relationships of EcDOS, a heme-regulated phosphodiesterase from *Escherichia coli*. *Acc Chem Res* **39:** 37–43.

Scheuermann, T.H., Tomchick, D.R., Machius, M., Guo, Y., Bruick, R.K., and Gardner, K.H. (2009) Artificial ligand binding within the HIF2α PAS-B domain of the HIF2 transcription factor. *Proc Natl Acad Sci USA* **106:** 450–455.

Schmitz, R.A., Klopprogge, K., and Grabbe, R. (2002) Regulation of nitrogen fixation in *Klebsiella pneumoniae and Azotobacter vinelandii*: NifL, transducing two environmental signals to the nif transcriptional activator NifA. *J Mol Microbiol Biotechnol* **4:** 235–242.

Söderbäck, E., Reyes-Ramirez, F., Eydmann, T., Austin, S., Hill, S., and Dixon, R. (1998) The redox-and fixed nitrogen-responsive regulatory protein NIFL from *Azotobacter vinelandii* comprises discrete flavin and nucleotide-binding domains. *Mol Microbiol* **28:** 179–192.

Taylor, B.L., and Zhulin, I.B. (1999) PAS domains: internal sensors of oxygen, redox potential, and light. *Microbiol Mol Biol Rev* **63:** 479–506.

Ukaegbu, U.E., and Rosenzweig, A.C. (2009) Structure of the redox sensor domain of methylococcus capsulatus (Bath) MmoS. *Biochemistry* **48:** 2207–2215.

Zoltowski, B.D., and Crane, B.R. (2008) Light activation of the LOV protein vivid generates a rapidly exchanging dimer. *Biochemistry* **47:** 7012–7019.

Zoltowski, B.D., Schwerdtfeger, C., Widom, J., Loros, J.J., Bilwes, A.M., Dunlap, J.C., and Crane, B.R. (2007) Conformational switching in the fungal light sensor vivid. *Science* **316:** 1054–1057.

Supporting information

Additional supporting information may be found in the online version of this article.

Please note: Wiley-Blackwell are not responsible for the content or functionality of any supporting materials supplied by the authors. Any queries (other than missing material) should be directed to the corresponding author for the article.